IJBPAS, February, 2020, 9(2): 292-309

ISSN: 2277–4998

International Journal of Biology, Pharmacy and Allied Sciences (IJBPAS)

'A Bridge Between Laboratory and Reader'

www.ijbpas.com

FORMULATION, CHARACTERIZATION AND OPTIMIZATION OF QUERCETIN LOADED CHITOSAN NANOPARTICLES BY EXPERIMENTAL DESIGN

RAVAL M*, PATEL P[1] AND SHETH N[2]

1: Department of Pharmaceutical Sciences, Saurashtra University, Rajkot

2: Gujarat Technological University, Ahmedabad

***Corresponding Author: E Mail: rmihir@yahoo.com**

Received 25th Aug. 2019: Revised 16th Sept. 2019: Accepted 10th Oct. 2019: Available online 1st Feb. 2020

https://doi.org/10.31032/IJBPAS/2020/9.2.4971

ABSTRACT

Purpose: The purpose of this study was to develop optimize and characterize Quercetin loaded chitosan (CS) nanoparticles.

Method: Chitosan nanoparticles of chitosan have been prepared using modified ionic gelation method. Box Behenken design with 15-runs was implemented. Polynomial equation, contour and 3D response surface plots were generated to relate the factors and responses. Prepared nanoparticles were characterized for particle size, Zeta potential, polydispersity index, entrapment efficiency, in-vitro release study along with FTIR, Differential scanning calorimetric and Scanning electron microscopy.

Result: It was proved that there was no any interaction showed between drug and excipients.A formulation showed prolonged drug release of up to 8 hrs by 45-52 %, smaller particle size, and narrow particle size distribution with good entrapment efficiency.

Conclusion: Processing parameters of chitosan nanoparticles were optimized by using box behenken design.

Keywords: Chitosan, Box Behenken Design, Ionic gelation method, Quercetin

INTRODUCTION

Nanoparticles are solid colloidal particles with diameters ranging from 1-1000 nm. They consist of macromolecular materials and which are therapeutically used as adjuvant in vaccines or as drug carriers, in which the active substance is dissolved, encapsulated, adsorbed or chemically attached. Nanoparticles can be made from a

wide range of materials, including proteins, polysaccharides and synthetic polymers. There are several studies have been suggested that nanoparticles systems can be preferably suited as a vehicle for sustained release therapy. **[1]**.

Polymeric nanoparticulate systems, biodegradable and biocompatible polymers are interesting for controlled drug delivery and drug targeting. Polymeric nanoparticles are solid, colloidal particles of 1 to 1000 nm in diameter. Polymeric nanoparticles having an advantages as compare to conventional formulations such as high stability, high specificity, high drug carrying capacity, produce controlled release, possibility to use in different route of administration and the capability to deliver both hydrophilic and hydrophobic drug molecules **[2]**. Among the different polymers, much attention has been paid to the nanoparticles made of biodegradable polymers such as chitosan (CS) due to its good biocompatibility, biodegradability, and novel drug release behaviour. Chitosan is the most important derivative of chitin, produced by removing the acetate moiety from chitin. Chitosan nanoparticles are potential delivery systems for vaccines, genes, and anticancer agents. Chitosan is a polysaccharide, similar in structure to cellulose **[3-8]**. Chitosan has many advantages specially for nanoparticles such as its ability to control the release of active agents, it avoids the use of hazardous organic solvents while fabricating particles since it is soluble in aqueous acidic solution, it is a linear polyamine containing a number of free amine groups that are readily available for crosslinking, its cationic nature allows for ionic crosslinking with multivalent anions along with its mucoadhesion nature **[9-12]**. The use of complexation between oppositely charged macromolecules to prepare chitosan nanoparticles has attracted much attention because the process is simple. In addition, reversible physical cross-linking by electrostatic interaction, instead of chemical cross-linking, has been applied to avoid the possible toxicity of reagents and other undesirable effects. Tripolyphosphate (TPP) is a polyanion, which can interact with the cationic chitosan by electrostatic forces.

QCT, or 3, 3′, 4′, 5, 7-pentahydroxyflavone, 1 of the 6 subclasses of flavonoids, has a wide range of biological activities. Quercetin, a widely distributed bioflavonoid, is well known to induce growth inhibition in a variety of human cancer cells. Quercetin glucuronides are the main circulating metabolites after dietary supplements with quercetin in humans. Quercetin is a plant-based flavonoid polyphenol and a super-antioxidant that is found in a broad spectrum of vegetables and fruits, such as green tea to grape skins,

apples and tomatoes. Quercetin is a strong chemoprotective natural compound for a wide range of cancers because of the multi-targeted way it relates to cancer cells in general. Quercetin strongly inhibited cell proliferation, and increased sub-G1 and apoptotic cell populations regardless of p53. Quercetin has the ability to stop the process that can turn healthy cells into malignant ones by protecting cellular DNA from mutations that can lead to cancer. Their biological activities mainly include electron transfer of free radicals, the activation of antioxidant enzymes, and the ability to inhibit oxidative stress **[13-17]**.

MATERIALS AND METHODOLOGY

Material

Quercetin was purchased from Sigma Aldrich, Mumbai (India), Chitosan (M.W 190-310 kDa) was gifted by Cognis Gmbh Pvt. Ltd. Germany, Sodium Tripolyphosphate (Cross-linking agent) and Tween 80 were purchased from sigma Aldrich, Mumbai (India), All other excipients, solvents were of pharmaceutical and analytical grade.

Method

Nanoparticle was prepared by modified ionic gelation method **[18]**. Different concentrations of chitosan (Medium Molecular weight, 190-310 kDa) was dissolved in 1% (v/v) Glacial acetic acid solution. Quercetin was dispersed in above solution with stirring condition at room temperature. Sodium tripolyphosphate solutions of different concentrations were prepared by dissolving in distilled water. Tween-80 (1%) was added as a surfactant. Sodium tripolyphosphate solutions was added drop wise to chitosan solution under constant magnetic stirring and stirring was continued for 1 hour. Chitosan nanoparticle suspension was centrifuged at 18,000 rpm for 20 min using Laboratory centrifuge and nanoparticles were collected. Supernatant was discarded by after confirmed the absence of free drug residue. The prepared nanoparticles were characterized in terms of particle size, Zeta Potential, Poly dispersity index and drug entrapment efficiency.

Optimization of formulation using Box-Behnken design

On the basis of preliminary trial batches, Concentration of chitosan (X1), Concentration of Sodium tripolyphosphate (X2) and Speed of homogenization (X3) were selected as independent variables and Particle size (Y1), Encapsulation Efficiency (Y2) and Drug Release at 8 Hr. (Y3) were selected as dependent variables (**Table 1**).

Box-behnken design with coded value and actual value was given in table and All the statistical evaluation with Box-Behnken design were carried out using Design Expert Software 7.0.0 trial version (Stat-EaseInc, Minneapolis, Minnesota). A statistical mathematical model terms was

utilized to evaluate responses as shown in equation 1.

$$Y = b_0 + b_1X_1 + b_2X_2 + b_3X_3 + b_{12}X_1X_2 + b_{13}X_1X_3 + b_{23}X_2X_3 + b_{123}X_{123}\, b_{11}X_{11} + b_{22}X_{22} + b_{33}X_{33} \quad (1)$$

Where, Y is the measured response, b_0 is the constant, b1, b2, b3 are the coefficient for the factor X1, X2,X3, b12, b23, b13, b123 are the coefficient of interaction b11, b22, b33 are the coefficients of the quadratic terms

All the batches were prepared according to the experimental design shown in **Table 2** summarizing an account of the 15 runs tested, their factor combinations, and the translation of the coded levels into the experimental units employed during the analysis.

Table 1: Transformation of coded value into actual value

Variables	Level of variables		
Independent variables	Low (-1)	Medium (0)	High (+1)
A = Concentration of chitosan (%w/v)	1	1:5	2
B = Concentration of STPP (%w/v)	0.5	0.6	0.7
C = Speed of homogenization (RPM)	10,000	15,000	20,000
Dependent variables; Y1 = Particle size (nm); Y2 = Entrapment efficiency (%); Y3 = Drug Release at 8 Hr.			

Table 2: Design matrix of Box-Behnken Design

Batch no	Independent variable Coded value			Independent variable (Real value)		
	X1 (%w/v)	X2 (%w/v)	X3 (RPM)	X1 (%w/v)	X2 (% w/v)	X3 (RPM)
B1	0	0	0	1.5	0.6	15000
B2	0	-1	-1	1.5	0.5	10000
B3	-1	0	-1	1	0.6	10000
B4	-1	-1	0	1	0.5	15000
B5	1	0	-1	2	0.6	10000
B6	-1	0	1	1	0.6	20000
B7	0	0	0	1.5	0.6	15000
B8	0	1	1	1.5	0.7	20000
B9	-1	1	0	1	0.7	15000
B10	0	1	-1	1.5	0.7	10000
B11	1	-1	0	2	0.5	15000
B12	1	1	0	2	0.7	15000
B13	0	0	0	1.5	0.6	15000
B14	0	-1	1	1.5	0.5	20000
B15	1	0	1	2	0.6	20000

Data optimization and validation of response surface methodology (RSM)

A multiple linear regression modeling approach was used to produce polynomial model including interaction and quadratic terms for all the response variables. The models were assessed on statistically significant coefficients and values of R2. The software constructs 3-D surface plots and 2-D contour plots. Two formulations were eventually selected as batches for checkpoints. The actual observed responses were compared with the predicted responses, and the measurement of percentage error. A linear regression plot was plotted between the real and expected reactions **[19, 20]**.

Characterization of Nanoparticle of Quercetin

Drug Excipient compatibility Study

Fourier Transforms Infrared Spectroscopy

This study was carried out by FTIR. Samples was kept in a sample holder of FTIR spectrophotometer (Nicolet IS 10, Thermo scientific) and scanned in the range of 400-4000 cm-1 at a resolution of 4 cm-1.

Differential Scanning Calorimetric study (DSC)

Differential scanning calorimeter measurements were carried out with a differential scanning calorimeter (DSC-60, TA 6OWS, Shimadzu) under nitrogen purging. DSC runs were conducted over a temperature range of 35 to 250 °C at 10°C/min under nitrogen flow rate of 100 ml/min.

Measurement of Particle size, Zeta potential and Polydispersity index (PDI)

Particle size, Zeta potential and PDI value of nanoprticle were determined using Zetatrac (MicrotracInc., USA).Every sample was diluted with distilled water. The surface charge (Zeta potential) was determined by measuring the electrophoretic mobility of the nanoparticles in the aqueous medium.

Measurement of Drug Entrapment Efficiency (DEE)

20 ml of suspension containing nanoparticles was centrifuged at 14000 rpm at 40 ^{0}C for 20 minutes. Nanoparticles were separated and supernant was collected. 1 ml of supernatant was diluted to 10 ml with Phosphate buffer pH 7.4 buffer solution. This solution was analyzed by UV-Visible Spectrophotometer at 253 nm. It expressed the amount of un-entrapped drug in the supernant. The Drug Entrapment Efficiency was calculated by following equation 2

$$\%\ \boldsymbol{Entrapment\ efficiency} = \frac{\mathbf{Da-Ds}}{\mathbf{Da}} * \mathbf{100} \text{ --------- (2)}$$

Where,

Da= Amount of drug added into formulation

Ds= Amount of un-entrapped drug

***In Vitro* drug release study**

The dialysis bag diffusion technique was used to perform *In vitro* drug release of the nanoparticle. Nanoparticles equal to 100 mg of Quercetin were filled in the dialysis bag and immersed in the 300 ml phosphate buffer pH 7.4 containing receptor chamber. Stirred at 100 RPM the system was maintained at 37 ± 0.50C.Five millilitre sample was withdrawn at predetermined time intervals and diluted appropriately. The absorbance was measured by UV-Visible spectrophotometer at 253 nm. The result of *in vitro* drug release from nanoparticles was analyzed using model dependent approach. Different kinetic models such as zero order, first order, higuchi, Hixson crowell, and webul model were applied to obtain the mechanism for drug release from chitosan nanoparticle.

Scanning electron microscopy (SEM)

The nanoparticles ' shape and surface morphology was visualized by scanning electron microscopy (SEM). 10 mg of the dried particle sample was mounted on a scanning electron microscopy stub (SEM). The stub was put into a sample holder and positioned in a scanning electron microscope vacuum chamber. The surface characteristics of the nanoparticles were observed.

RESULTS AND DISCUSSION

Chitosan nanoparticles have been successfully prepared using modified ionic gelation method with several advantages compared with other solvent-based preparation methods due to the absence of non-toxic solvent, higher yield, better entrapment and easier process.

Drug – Excipient Compatibility study

Fourier Transform Infra Red Spectroscopy (FT-IR)

The FTIR spectrum of Quercetin (A) was shown in **Figure 1**. All the principal peaks were found in the FTIR spectra of the Quercetin (A) which indicate that the drug was in the pure form. Various absorption bands within the 4000-400 cm-1 range were recorded in the FTIR spectra of chitosan, Different stretching vibration bands were observed in the range 3425-2881 cm-1 related to(N-H) in (NH2) assoc. in primary amines **[21, 22, 23]**. The band at 3425-3422 cm-1 could beassigned to (N-H), (O-H) and (NH2) which present in chitosan in different amounts, among which NH2 groups being the least Moreover, within the 1300-1200 cm-1 region, the absorption bands at 1262 cm-1 and 1205 cm-1 were observed, which could be assigned to complex vibrations of NHCO, with characteristic frequencies for secondary amides only **[24]**.

Physical mixture of Drug and Polymer shows same peaks that indicate there was no interaction between drug and excipient. Quercetin loaded formulation of nanoparticles shows complete disappearances of Quercetin's characteristic peak; a fact that the drug was molecularly dispersed within the polymer matrix and shows the same Polymer peak. FT-IR spectra of Quercetin, Chitosan, Physical mixture and Quercetin loaded nanoparticle formulation shows in **Figure 1A, 1B, 1C, 1D** respectively.

Differential Scanning Colorimetery (DSC):

The pure Quercetin DSC thermogram indicates large endothermic peak at 318.49 ° C, which corresponds to its melting point. The chitosan DSC thermogram showed an endothermal peak between 82.48 -84.34oC and an exothermic peak between 190.25 -192.68oC as shown in **Figure 2**. The endothermic peak also called the temperature of dehydration (TD), is

attributed to the water loss associated with chitosan hydrophilic groups **[25, 26]**. Nanoparticulate formulation DSC thermogram shows complete disappearing of Quercetin's characteristic peak; a fact that the drug was molecularly disperded within the polymeric matrix. The DSC curve Quercetin and Quercetin loaded nanoparticles shows in **Figure 2A and 2B** respectively.

POLYMERIC NANOPARTILCE

Ionic Gelation Method

The CSNPs are formed due to the electrostatic interaction between positively charged amine group of chitosan and negatively charge group of polyanion such as tripolyphosphate. This technique offers a simple and mild preparation method in the aqueous environment **[27]**.

Optimization of formulation using Box-Behnken design

Nanoparticles were optimized by Box behenken design and results of independent variables are shown in below **Table 3**.

Effect on Particle Size

If increase in conc.of chitosan lower to high, lead to increase in the particle size due to the larger emulsion droplets are formed when chitosan concentration was high and this will lead to the formation of larger particle. Particle size was reduces with increase in TPP concentration because higher amount of cross linking agent hardens the chitosan nanoparticle and formed the small rigid matrix. The DEE, particle size, zeta potential and PDI of all 15 batches were shown in **Table 3**. Increasing homogenization speed decreases particle size because higher speed inhibits particle aggregation and produces gravitational forces in the homogenization gap resulting in decreased nanosize liquid droplet. Zeta potential was increase with increase in speed of homogenization due to the higher mechanical force was present and lead to the lower amount of anionic molecule was adsorbed on nanoparticle surface. 3D Plot and Contour plot for particle size shown in **Figure 3**.

Effect on Entrapment Efficiency

The DEE, particle size, zeta potential and PDI of all 15 batches were shown in table 3. If increase in conc^{n} of chitosan lower to high, lead to increase in the DEE because of presence of higher amount of chitosan increase in matrix density. If increase in TPP concentration lower to high, increase in entrapment efficiency due to the more amount of TPP could cross link greater amount of chitosan and hence entrap the higher amount of drug. The DEE was found to be decrease with increase in speed of homogenization due to the formation of small particle and hence small amount of drug should be entrapping in the

nanoparticle.3D Plot and Contour plot for Entrapment efficiency shown in **Figure 4**.

Effect on Drug Release at 8 Hrs.

The results of in vitro studies suggested a significant decrease in the rate and extent of drug release with an increase in polymer concentration, which may be due to an increase in polymer matrix, gel strength, and the formation of gel layer with a longer diffusion path, resulting in a reduction in the drug diffusion coefficient.As shown in Figure 8, the release rate of Quercetin increased as the amount of TPP increased. The effect of homogenization time on the drug release was evaluated for Nanoparticle. There is no significant difference were observed between them as in the particle size results. The release of quercetin prepared at three different homogenization speeds. The drug release from the nanoparticle prepared at higher speed was higher than the formulations prepared with lower speed.This finding was attributed to the smaller particle size of the formulation. While decrease in the size of nanoparticle, an increase in drug release was obtained. 3D Plot and contour plot were shown **Figure 5 [28]**.

Fitting of the data to the Model

The optimum formulation of NPs loaded with quercetin was selected based on achieving minimum particle size, maximum entrapment efficiency and drug release. Using Design –Expert software, all the response observed for 15 formulations prepared were fitted simultaneously to first order, second order and quadratic model. It was observed that best fitted model was Quadratic for all response Y1 (Particle size), Y2 (Entrapment efficiency) and Y3 (Drug release at 8 Hr)

A stepwise multivariate linear regression was performed to evaluate the observations. The statistical evaluation of the result was carried out by Analysis of Variances (ANOVA)

Table 4 illustrates the fitted polynominal equation (Full model) relating to the transformed factors. The polynominal equation could be used to draw a conclusion after considering the magnitude of the coefficient and mathematical sign, i.e. positive or negative, that it carried. The Full model word having a significant p value ($p < 0.05$).

The result of ANOVA, performed to identify insignificant factors. Here, Fcal is less than Ftab for all response such as Particle size, Entrapment efficiency and drug release at 8 Hrs.. So, model is valid for both. Result of ANOVA shown in **Table 5.**

Optimization and Validation of model:

For optimization of model Overlay plot shows in **Figure 6**.

Check point batches obtained from extensive grid search. Check point batch CP1 was formulated using Chitosan

concentration 0.42, TPP concentration 0.65 and Homogenization speed 18625 RPM having predicted Particle size 315.57 nm and Entrapment efficiency 41.69% and drug release after 8 Hr. 9.33. Actual Particle size 316.5 nm and Entrapment efficiency 40.23% and drug release at 8 Hr 9.65% respectively that shows error less than 8%.**(Table 6)** Graph of Actual value of Particle size shows in **Figure 7**.

% Yield, Drug content, Zeta potential and PDI

Results of physicochemical characterization of Quercetin loaded Chitosan nanoparticles were shown in **(Table 7)**.

TThe average yields of nanoparticles were about 48.26 ± 2.01% to 56.36 ± 0.45%. The average loading in the formulations were found to increase with an increase in polymer concentration used in the formulations. PDI value of all batches are less than 1, Hence it's indicate uniformity of particles in all batches. The results showed quercetin loaded chitosan nanoparticles had zeta potential value of 22.3±0.98 to 37.4±1.56 mV. The positive surface charge of all formulations may be due to the use cationic polyelectrolyte (Chitosan) and the addition of STPP in the formulation aids to reduce aggregation of nanoparticles may indicate the good stability of the formulations **[29]**.

Drug Release

Release studies were carried out by using three different release medium, phosphate buffers at pH 7.4,

Likewise, this result suggests that due to the partition of the drug into the surface-active agent layer adsorbed at the droplet surface some of the drug is localized on the surface of the nanoparticles. After this initial burst, drug release is Show in sustained release pattern, and around 76% drug release at 8 hrs as per depicted in **Figure 8.**

Scanning electron Microscopy

Scanning electron microscopy was performed to identify the morphology of the optimized Nanoparticles. Scanning electron microscopy image of Nanoparticles **(Figure 9)** had shown that particles are smooth and spherical in shape.

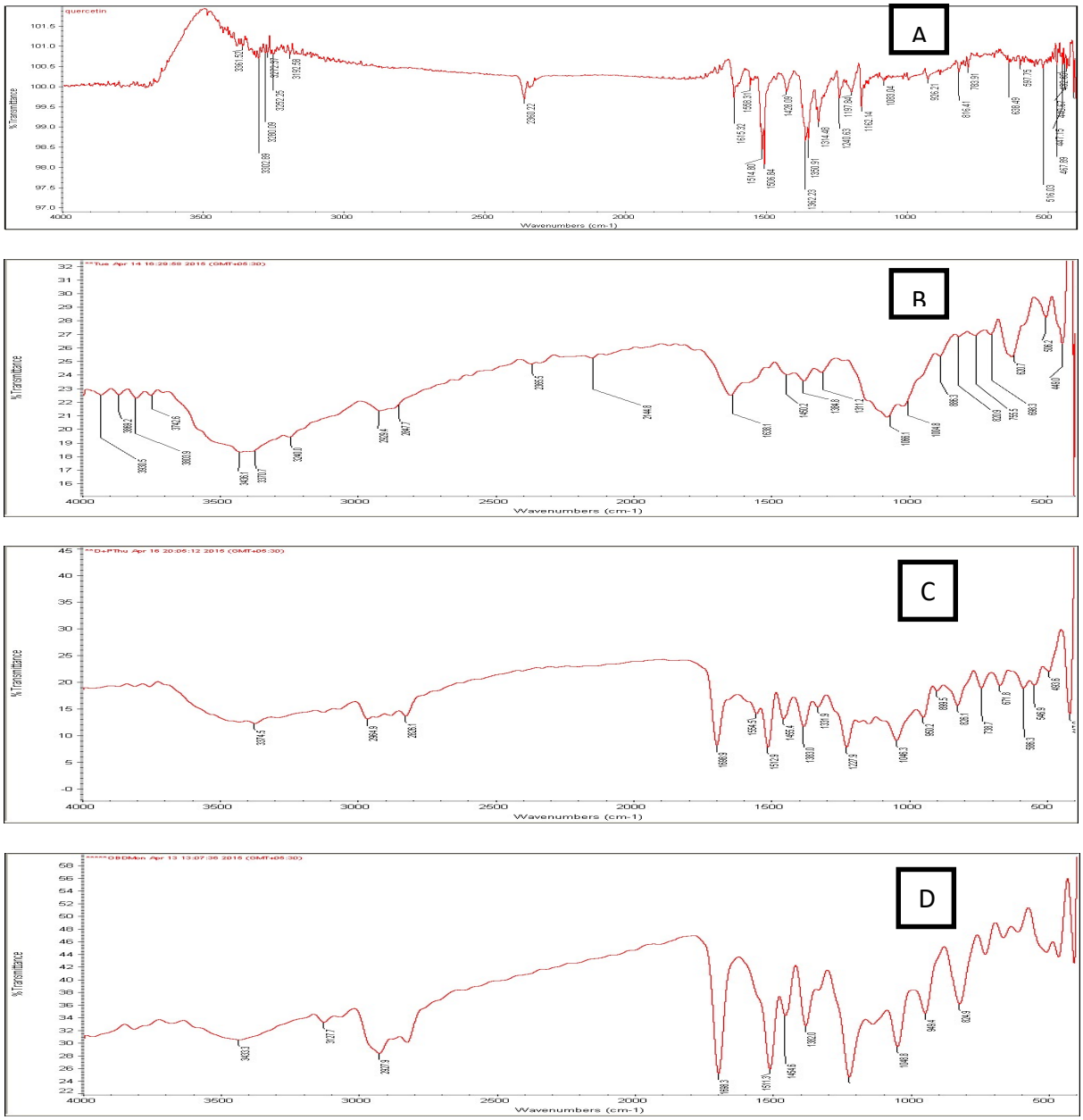

Figure 1: FTIR Spectra of A) Quercetin, B) Chitosan, C) Physical mixture and D) Formulations

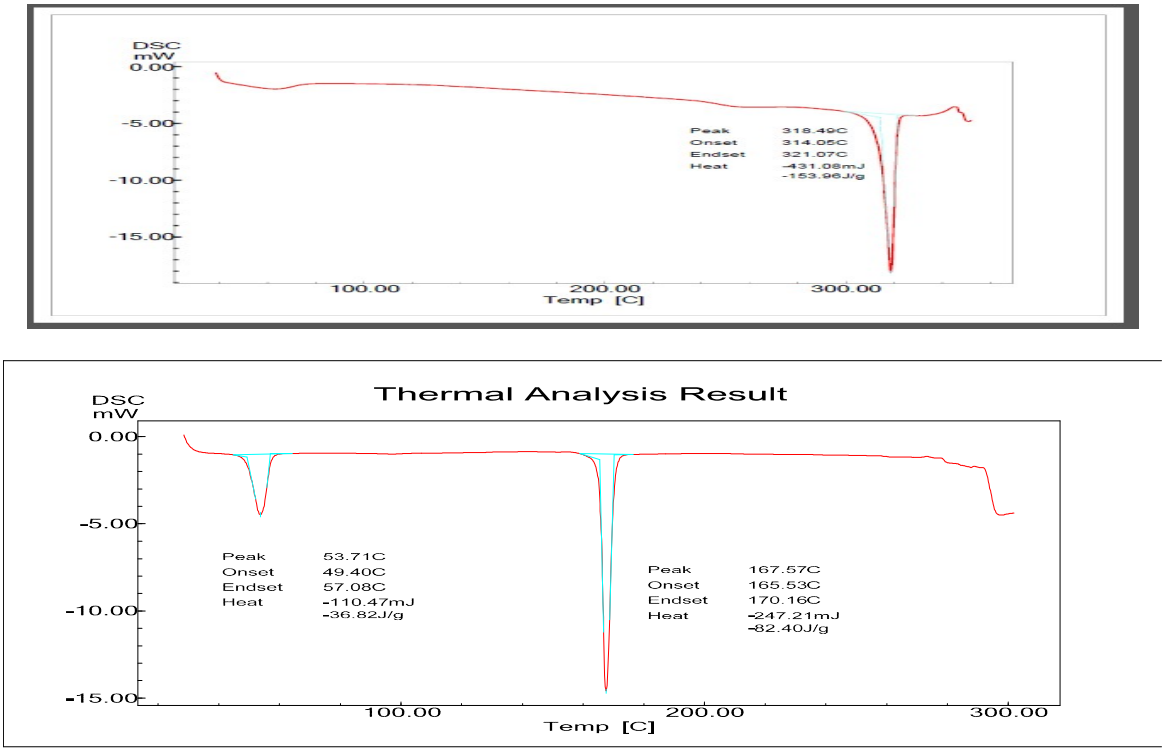

Figure 2: DSC Thermogram of A) Quercetin, B) Formulations

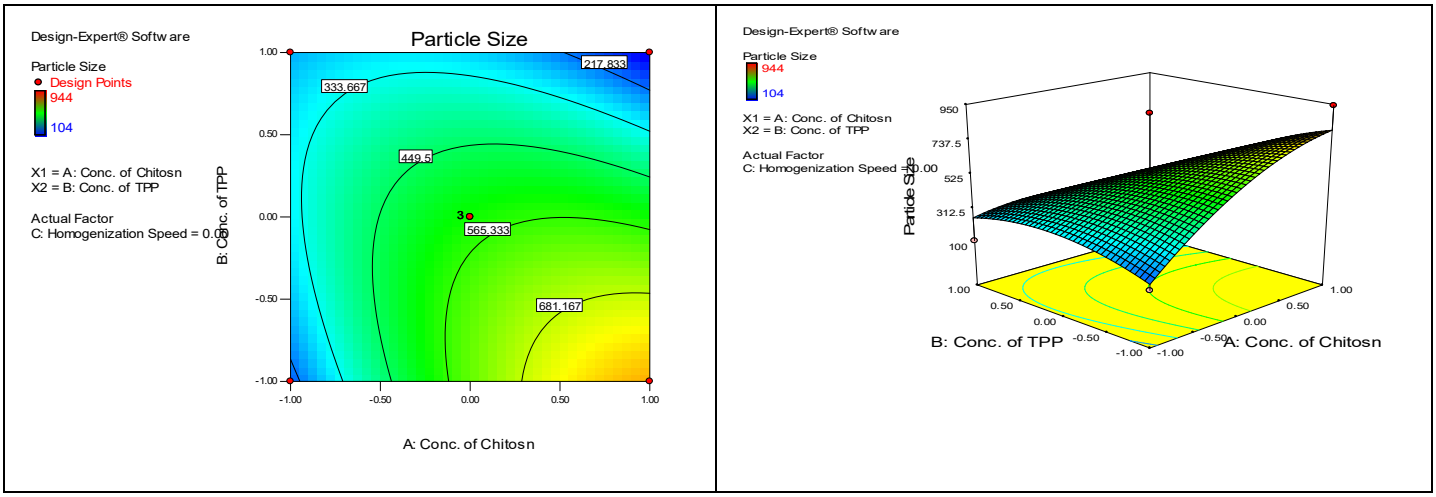

Figure 3: 3D and over lay plot for Particle Size

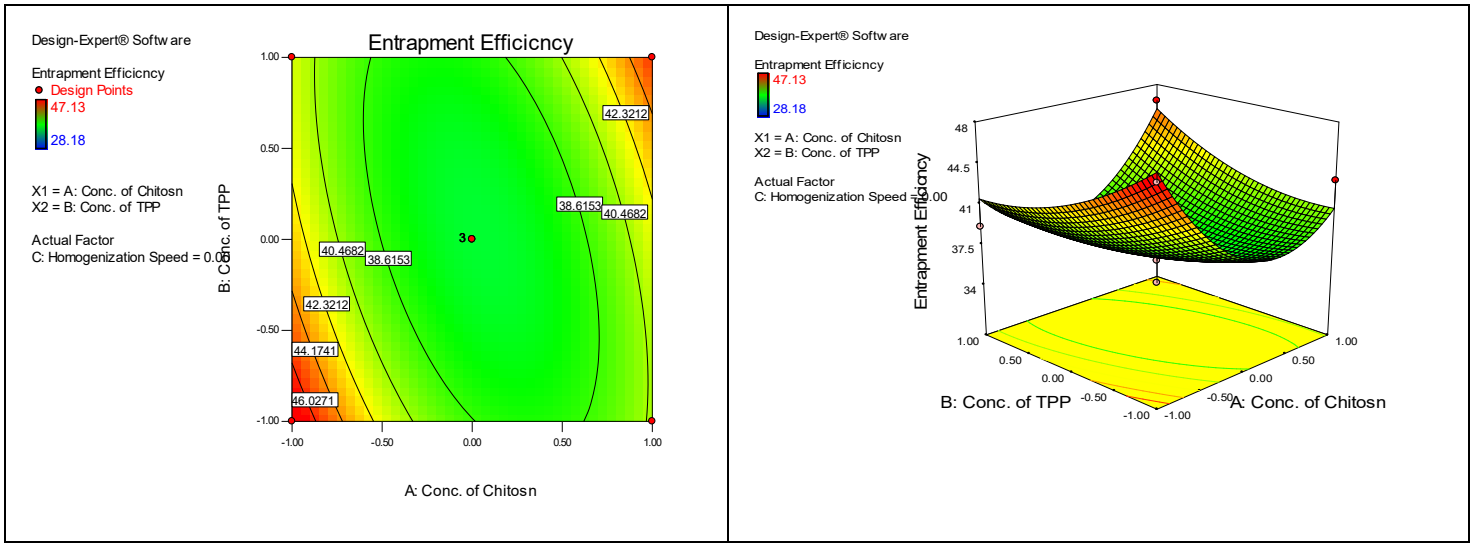

Figure 4: 3D and over lay plot for Entrapment Efficiency

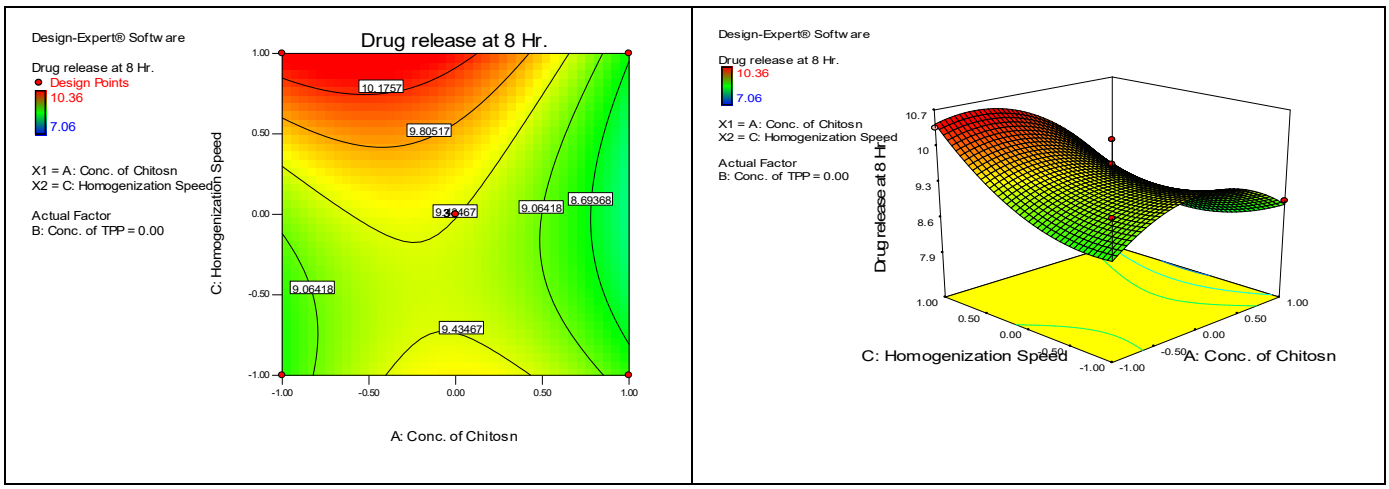

Figure 5: 3D and over lay plot for Drug Release at 8 Hr

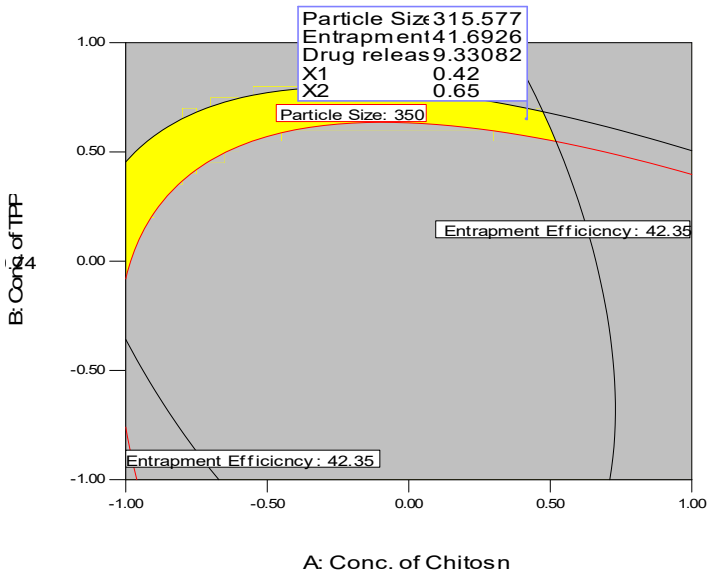

Figure 6: Overlay plot for selection of Checkpoint batch

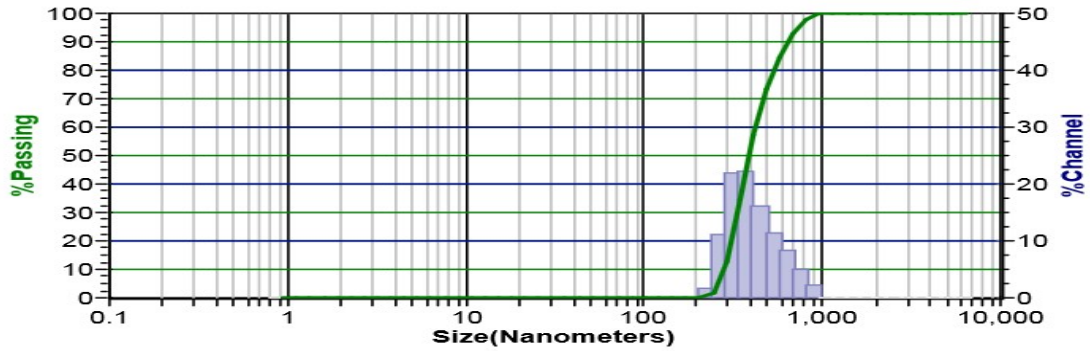

Figure 7: Particle Size distribution graph

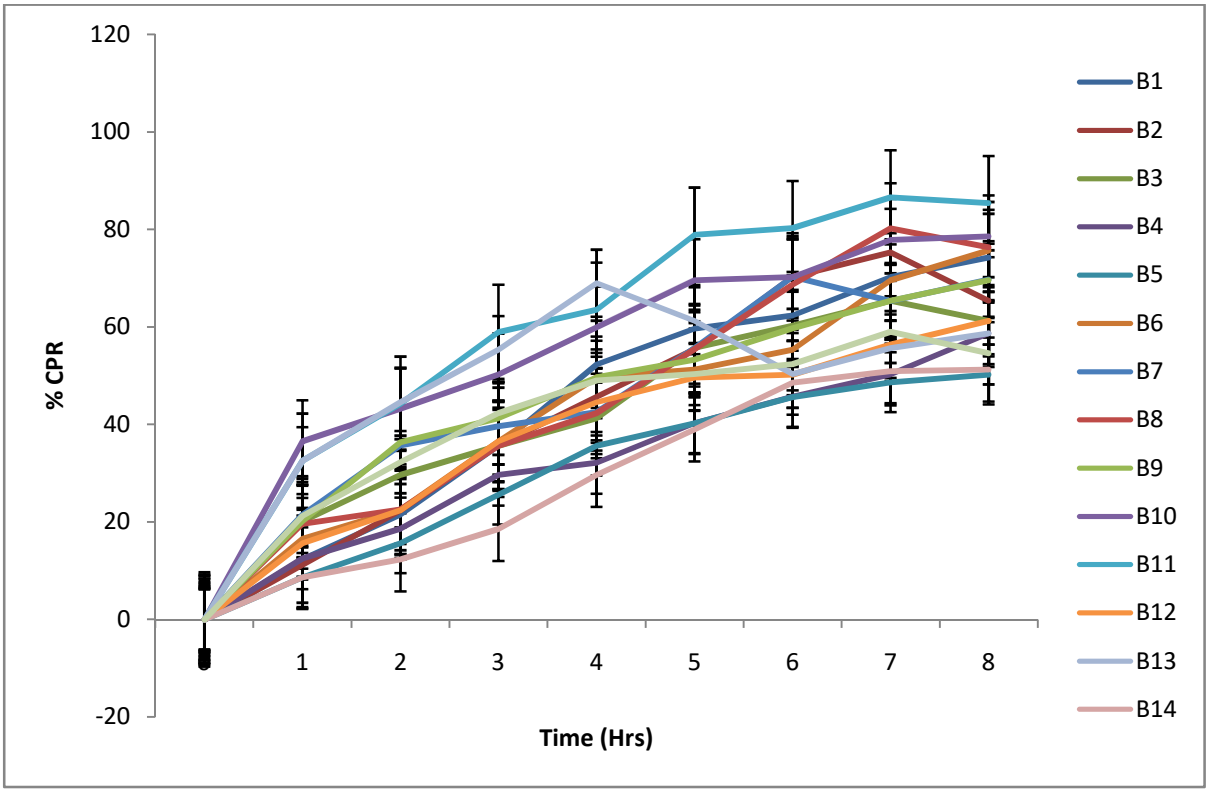

Figure 8: Drug Release of all batches

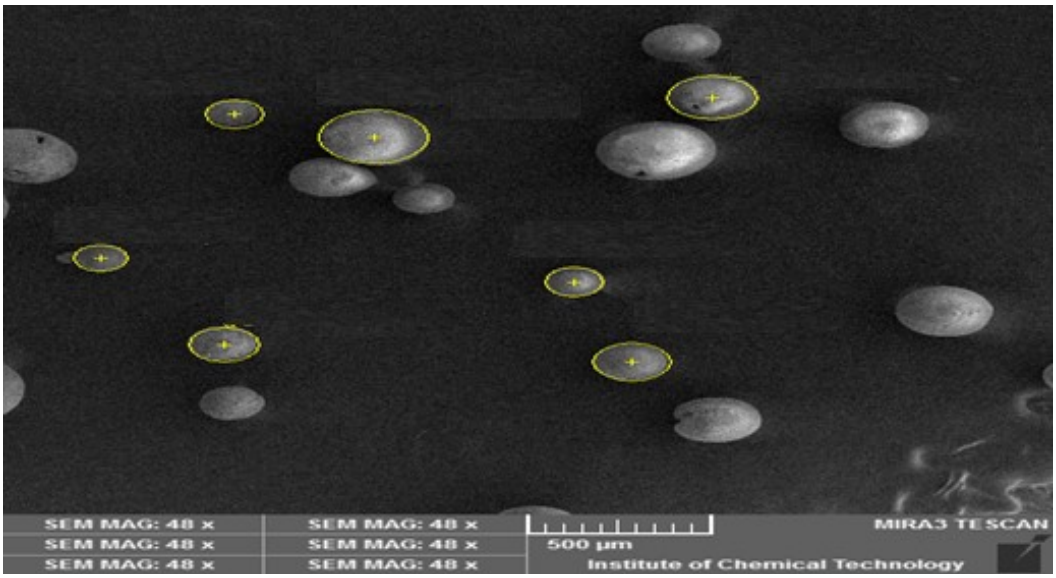

Figure 9: Scanning Electron Microscopy of Optimized Nanoparticle formulations

Table 1: Transformation of coded value into actual value

Variables	Level of variables		
Independent variables	**Low (-1)**	**Medium (0)**	**High (+1)**
A = Concentration of chitosan (%w/v)	**1**	**1:5**	**2**
B = Concentration of STPP (%w/v)	**0.5**	**0.6**	**0.7**
C = Speed of homogenization (RPM)	**10,000**	**15,000**	**20,000**
Dependent variables; Y1 = Particle size (nm); Y2 = Entrapment efficiency (%); Y3 = Drug Release at 8 Hr.			

Table 2: Design matrix of Box-Behnken Design

Batch no	Independent variable Coded value			Independent variable (Real value)		
	X1 (%w/v)	X2 (%w/v)	X3 (RPM)	X1 (%w/v)	X2 (% w/v)	X3 (RPM)
B1	0	0	0	1.5	0.6	15000
B2	0	-1	-1	1.5	0.5	10000
B3	-1	0	-1	1	0.6	10000
B4	-1	-1	0	1	0.5	15000
B5	1	0	-1	2	0.6	10000
B6	-1	0	1	1	0.6	20000
B7	0	0	0	1.5	0.6	15000
B8	0	1	1	1.5	0.7	20000
B9	-1	1	0	1	0.7	15000
B10	0	1	-1	1.5	0.7	10000
B11	1	-1	0	2	0.5	15000
B12	1	1	0	2	0.7	15000
B13	0	0	0	1.5	0.6	15000
B14	0	-1	1	1.5	0.5	20000
B15	1	0	1	2	0.6	20000

Table 3:Results for particle size (Y1), Entrapment efficiency (Y2) and CDR at 8 Hrs

Batch No.	Chitosan Conc. $X_{1\,(\%)}$	STPP Conc. $X_{2\,(\%)}$	Homogenization Speed $X_{3\,(RPM)}$	Particle Size (nm)	EE (%)	CDR at 8 Hr (%).
1	1	0.7	15000	899±0.12	34.12±1.02	74.25±1.21
2	1.5	0.5	10000	678±0.33	39.15±1.23	65.32±1.54
3	2	0.5	15000	410±0.82	40.12±0.56	61.25±0.65
4	1	0.6	10000	156±0.78	47.13±0.98	58.65±0.45
5	1	0.6	20000	419±0.64	44.59±0.55	50.21±1.56
6	1.5	0.5	20000	104±0.45	41.89±0.42	75.63±1.21
7	2	0.6	20000	319±0.32	36.12±0.22	69.67±0.36
8	1	0.5	15000	210±0.25	29.12±1.02	76.36±0.77
9	1.5	0.6	15000	108±0.11	39.12±1.56	69.55±0.54
10	2	0.7	15000	184±0.72	41.15±0.69	78.56±1.32
11	1.5	0.7	10000	944±0.64	43.12±1.21	85.36±0.89
12	1.5	0.7	15000	137±0.65	46.52±0.25	61.25±0.65
13	2	0.6	10000	388±0.54	40.13±0.36	58.63±2.12
14	2	0.6	15000	123±2.20	29.1±0.68	51.23±1.25
15	2	0.6	15000	184±1.25	28.18±0.87	54.56±0.25

Table 4: Result of Regression Analysis

Particle Size (nm)	B_0	B_1	B_2	B_3	B_{12}	B_{13}	B_{23}	B_1^2	B_2^2	B_3^2
FM	53.35	11.25	-15.7	-13.3	-18.9	7.75	14.52	-10.9	-8.97	-14.6

Entrapment efficiency (%)	B_0	B_1	B_2	B_3	B_{12}	B_{13}	B_{23}	B_1^2	B_2^2	B_3^2
FM	36.79	-0.731	-0.323	-4.59	2.852	-4.54	-0.49	5.62	1.55	-3.71

Drug Release at 8 Hr.	B_0	B_1	B_2	B_3	B_{12}	B_{13}	B_{23}	B_1^2	B_2^2	B_3^2
FM	9.44	-0.413	0.645	0.366	-0.157	-0.435	-0.512	-0.704	-0.77	0.480

Table 5: Result of ANOVA

Particle size		Df	SS	MS	F value	R^2 value
Regression	FM	9	35.58	19.76	4.63	0.9852
Residual	FM	7	18.56	22.62	2.12	0.9645
Entrapment efficiency		**Df**	**SS**	**MS**	**F value**	**R^2 value**
Regression	FM	10	55.16	12.13	5.05	0.9597
Residual	FM	9	12.13	32.15	3.23	0.8924
Drug Release at 8 Hr.		**Df**	**SS**	**MS**	**F value**	**R^2 value**
Regression	FM	10	42.13	12.39	4.21	0.9227
Residual	FM	7	11.21	29.35	2.23	0.8952

ANOVA: Analysis of Variance, df: Degree of Freedom, SS: Sum of Square, MS: Mean of Square, F: Fischer's ratio, R: Regression coefficient, FM: Full model

Table 6: Composition of Check point batch

Batch no.	X_1 (%)	X_2 (%)	X_3 (RPM)	Response	Actual value	Predicted value	% Error
CP_1	0.42	0.65	18625	Y_1	316.5 nm	315.57 nm	0.29
				Y_2	40.23%	41.69%	3.62
				Y3	9.65%	9.33%	3.31

Table 7: Physiological parameters of all batches

Batch No.	PDI	Zeta Potential	Pdt Yield (%)
1	0.22	24.9±0.32	57.60±0.66
2	0.244	27.9±0.66	57.29±1.12
3	0.259	24.1±1.45	50.34±0.54
4	0.168	35.1±1.36	52.80±2.10
5	0.25	32.5±0.65	62.21±1.02
6	0.11	37.4±1.56	52.52±0.92
7	0.246	32.8±2.25	51.23±0.65
8	0.21	28.9±0.65	54.21±0.47
9	0.212	35.3±1.05	49.25±1.52
10	0.181	22.3±0.98	48.26±2.01
11	0.179	28.4±0.45	63.25±1.25
12	0.195	24.7±2.25	61.23±0.85
13	0.209	29.8±0.56	56.36±0.45
14	0.185	30.2±1.25	55.32±0.36
15	0.221	34.4±0.22	59.89±0.25

CONCLUSION

In the current research, the effect of some process variables on the particle size, entrapment efficiency, and in vitro drug release of the Nanoparticles of quercetin was studied by Box Behenken design. The lower Particle size, higher drug release, and higher entrapment of drugs can be obtained by enhancing the concentration of polymer, enhancing the

concentration of STPP and optimize the homogenization speed.

Acknowledgment

Acknowledge to Cognis Gmbh Pvt. Ltd. Germany for providing chitosan as a gift sample.

REFERENCES

[1] VJ Mohanraj, Y Chen, Nanoparticles – A Review, Tropical Journal of Pharmaceutical Research, June 2006; 5 (1): 561-573

[2] Singh R, Lillard JW Jr. Nanoparticle-based targeted drug delivery. Exp Mol Pathol. 2009; 86(3): 215–223.

[3] Serpe. L, Catalano. M, Cavalli. R, Ugazio. E, Basco. O, Canaparo.R, Munton.E, Friaria.R, Grasco. M.R, Eandi. M, Zara. G.P, Cytotoxicity of anticancer drugs incorporated in solid lipid nanoparticles on HT-29 colorectal cancer cell line. Eur.J. Pharm and Biopharm. 2009; 58: 673-680.

[4] Yesim Aktas, Andrieux. K, Alonso. M.J, Calvo.P, Gurso. R.N, Couvreu. Pr, Capan.Y, Perparation and in vitro evaluation of chitosan nanoparticles containing a caspase inhibitor. Int .J. Pharm. 2005; 298: 378-383. 4.

[5] Colona. C, Conti. B, Perugini. P, Pavanatt. F, Modena. T, Dorat. R, Iad Arola. D, Genta.I, Exvivo evaluation of prolidse loaded chitosan nanoparticles for the enzyme replacement therapy. Eur. J. Pharm and Biopharm. 2008;70: 58-65.

[6] Bodmeier, Park. J.S, Han. T.H, Lee.K.Y, Han. S.S, Hwang. J.J, Moon. D.H, Kim. S.Y, N.acetylhistidine-conjugated glycol chitosan self-assembled nanoparticles for intracytoplasmic delivery of drugs: Endocytosis, exocytosis and drug release, J. Control. Rel. 2006; 115: 37-45.

[7] Dong-won Lee, Powers.K, Bane.R, Physicochemical properties and blood compatibility of acylated chitosan nanoparticles. Carbohydrates Polymers. 2004;58: 371-377.

[8] Ana Vila, Sanchez. A, Jsabel.k, Kisse.T, Jato.J. L.V, Alonso.M.J, Low moleculer weight chitosan nanoparticles as new carriers for nasal vaccire delivery in mice. Eur. J. Pharm and Biopharm. 2003; 57: 123-131.

[9] Yang.W, Zheng.Y, Wang.C, Hu.J, Fu.S, Dong.L, Wu.L, Shen.X, nanoparticles based on the complex of chitosoan and polyaspartic acid sodium salt: Preparation, characterization and the use of 5flurouracil delivery. Eur J. Pharm and Biopharm. 2007;67: 621631

[10] Yan Wu, Yang.W, Wang. C, Hu. J, Fu.S, Chitosan nanoparticles as a novel delivery system for ammonium glycyrrizinate. Int. J. Pharm. 2005; 295: 235-245.

[11] Du.Y, Wang. Q, Zhang. N, Hu. X, Yang. J, Chitosan/starch fibres and their properties for drug controlled release, Eur.J.Pharm and Bio pharm. 2007; 66: 398-404.

[12] Dadashazadeh. S, Derakhashandeh. K, Erfan. M., Encapsulation of 9-nitro-camphothecin, a novel anticancer durg, in biodegradable nasnoparticles: Factorial design, characterization and release Kinetics. Eur J. Pharm and Biopharm. 2007; 66: 34-41.

[13] Salvamani S, Gunasekaran B, Shaharuddin NA, Ahmad SA, Shukor MY. Antiartherosclerotic effects of plant flavonoids. Biomed Res Int 2014. Article ID 480258.

[14] Sultana B, Anwar F. Flavonols (Kaempeferol, quercetin, myricetin) contents of selected fruits, vegetables and medicinal plants. Food Chem. 2008;108:879–84.

[15] Parasuraman S, Maithili KS. Antioxidant and drug metabolism. Free. Radic. Antioxid. 20 14; 4:1–2.

[16] Pham-Huy LA, He H, Pham-Huy C. Free radicals, antioxidants in disease and health. Int J Biomed Sci. 2008;4:89–96.

[17] Valko M, Leibfritz D, Moncol J, Cronin MT, Mazur M, Telser J. Free radicals and antioxidants in normal physiological functions and human disease. Int J Biochem Cell Biol. 2007; 39: 44–84.

[18] Gupta M, Marwaha RK, Dureja H., Development and Characterization of Gefitinib Loaded Polymeric Nanoparticles by Ionic Gelation Method. Pharm Nanotechnol. 2017; 5(4): 301-309

[19] Yasir M, Sara UVS, Som I, Haloperidol Loaded Solid Lipid Nanoparticles for Nose to Brain Delivery: Stability and In vivo Studies. J Nanomedic Nanotechnol, 2015.

[20] Guo W, Quan P, Fang L, Sustained release donepezil loaded PLGA microspheres for injection: preparation, *in vitro* and *in vivo* study. Asian J Pharm Sci. 2015;10:405–414.

[21] Dunkan, A. B. F., W. Gordy, R. N. Jones, F. A. Matsen, C. Sandorfy, W. West, Chemical Application of Spectroscopy, Interscience Publ., London, 1956, 448-466.

[22] Shigemassa, Y., H. Matsuura, H. Sashiwa, H. Saimoto, International J. Biological Macromolecules, 2006, 18, 237

[23] Spasov, S., A. Arnaudov, Application of Spectroscopy in Organic Chemistry, Nauka i Izkustvo, Sofia, 1978, 107-115, 151-156.

[24] Furniss B., Hannaford A., Smith P., Thatchell A.: Text Book of Practical Organic Chemistry, 5thedn., pp. 695–698. Longman Scientific and Technical, Harlow, 1989.

[25] M. K. Cheung, K. P. Wan and P. H. Yu, Miscibility and morphology of chiral semicrystalline poly-(R)-(3-hydroxybutyrate)/ chitosan and poly-(R)-(3-hydroxybutyrate-co-3-hy

droxyvalerate)/ chitosan blends studied with DSC, 1H T1 and T1ρ CRAMPS, Journal of applied polymer science, 2002; 86(5): 1253-1258.

[26] F. Kittur, K. H. Prashanth, K. U. Sankar and R. Tharanathan, Characterization of chitin, chitosan and their carboxymethyl derivatives by differential scanning calorimetry, Carbohydrate polymers, 2002, 49(2), 185-193.

[27] Megha Agarwal, Nagar D. P., Nalini Srivastava, MK Agarwal, Chitosan Nanoparticles based Drug Delivery: An Update., International J. Advanced Multi disciplinary Research, 2015, 2(4): 1–13.

[28] Badıllı U, Sen T, Tarımcı N. Microparticulate Based Topical Delivery System of Clobetasol Propionate., AAPS Pharm Sci Tech. 2011; 12(3): 949-57

[29] Honary S, Zahir F. Effect of zeta potential on the properties of nanodrug delivery systems—a review (Part 1). Trop J Pharm Res. 2013; 12(2):255–64.